1 Name

Damian Rybicki

2 Degrees, titles - with year, institution and title of PhD thesis.

- M. Sc. - 2002 at the Faculty of Physics and Applied Computer Science of the AGH University of Science and Technnology in Krakow, Poland
- PhD (with honorable mention) 2007, *"Nuclear magnetic resonance study of selected Ruddlesden-Popper manganites"*, Faculty of Mathematics and Physics, Charles University, Prague, Czech Republic and Faculty of Physics and Applied Computer Science of the AGH University of Science and Technology in Krakow, Poland (PhD studies were part of EU RTN SCOOTMO).

3 Employment history.

- 2011-up to now: assistant professor at the Faculty of Physics and Applied Computer Science of the AGH University of Science and Technology in Krakow, Poland
- 2007-2014: post-doctoral researcher at the Universität Leipzig, Fakultät für Physik und Geowissenschaften
- 2007-2010: teaching assistant at the Faculty of Physics and Applied Computer Science of the AGH University of Science and Technology in Krakow, Poland

4 Achievement

4.1 Title

Electronic spin and charge properties of high-temperature superconductors and manganese perovskites

4.2 Publications constituting scientific achievement

O1. M. Jurkutat, D. Rybicki, O. P. Sushkov, G. V. M. Williams, A. Erb, J. Haase, *"Distribution of electrons and holes in cuprate superconductors as determined from ^{17}O and ^{63}Cu nuclear magnetic resonance"*, 2014, Phys. Rev. B vol. 90, 140504

O2. D. Rybicki, M. Jurkutat, S. Reichardt, Cz. Kapusta, J. Haase, *„Perspective on the phase diagram of cuprate high-temperature superconductors"*, Nature Commun., 2016, vol.7, 11413

O3. J. Haase, D. Rybicki, C. P. Slichter, M. Greven, G. Yu, Y. Li, X. Zhao, *"Two-component uniform spin susceptibility in superconducting $HgBa_2CuO_{4+\delta}$ single crystals measured using ^{63}Cu and ^{199}Hg nuclear magnetic resonance"*, 2012, Phys. Rev. B vol. 85, 104517

O4. D. Rybicki, J. Kohlrautz, J. Haase, M. Greven, X. Zhao, M.K. Chan, C. J. Dorow, and M. J. Veit, *"Electronic spin susceptibilities and superconductivity in $HgBa_2CuO_{4+\delta}$ from nuclear magnetic resonance"*, 2015, Phys. Rev. B vol. 92, 081115(R)

O5. D. Rybicki, J. Haase, M. Greven, G. Yu, Y. Li, Y. Cho, X. Zhao, *„Spatial Inhomogeneities in Single-Crystal $HgBa_2CuO_{4+\delta}$ from ^{63}Cu NMR Spin and Quadrupole Shifts"*, 2009, J. Supercond. Nov. Magn. vol. 22, 179

O6. D. Rybicki, T. Meissner, G. V. M. Williams, S. V. Chong, M. Lux, J. Haase, *"^{75}As NMR study of overdoped $CeFeAsO_{0.8}F_{0.2}$"*, 2013, J. Phys.: Condens. Matter vol. 25, 315701

O7. J. M. Michalik, D. Rybicki, Z. Tarnawski, M. Sikora, J. de Teresa, M. Ibarra, C. Kapusta, *„^{55}Mn NMR observation of colossal magnetoresistance effect in $Sm_{0.55}Sr_{0.45}MnO_3$"*, 2017, Journal of Physics: Condensed Matter vol. 29, 265802

O8. D. Rybicki, M. Sikora, J. Przewoznik, Cz. Kapusta, J. F. Mitchell, *„Interplay of local structure, charge, and spin in bilayered manganese perovskites"*, 2018, Phys. Rev. B, vol. 97,115158

4.3 Discussion of results and significance of above mentioned publications

4.3.1 Introduction

Every day hundreds of new devices, materials or solutions are presented on the market. It is of course a result of amazing human intellect, but it would be impossible without rapid technological progress, which requires constant development of more and more advanced and complicated devices and materials. Among the latter a special attention is given to superconductors and novel magnetic materials. While magnetic materials are known since centuries and are in broad use, applications of superconductors are very limited mostly due to the fact that they superconduct only at temperatures much lower than room temperature. Nevertheless, they are still studied with the aim to fully understand the nature of superconductivity and, of course, to create materials with higher critical temperatures (T_c) in order to to be able to use them in every day life e.g. for lossless electrical energy transfer.

Currently, the highest T_c values (at ambient pressure) are achieved by so called high-temperature superconducting cuprates. However, for the past 20 years there has been no progress in synthesizing cuprates with higher T_c values. Up to now, there is no theory starting from the first principles, which could reliably predict T_c values, not to mention ability to explain all phenomena observed in the cuprates such as e.g. the pseudogap or charge density fluctuations. In order to advance our understanding one has to look at all families of cuprates, which, despite many similarities, show significantly different structural or electronic properties, e.g. T_c values. There are only a few relations, which describe all cuprate families and finding new ones could lead to progress in research not only on cuprates, but in other materials, since similar phenomena and interactions are present in all systems with correlated electrons. The first step appears to be the identification, which material parameters are responsible for setting T_c values and how to change them, to create materials, which could superconduct at temperatures higher than achieved so far.

4.3.2 Phase diagram of all cuprates based on NMR. [Publications O1-O2]

The cuprates' essential building blocks are the CuO_2 plane and charge reservoir (CR) layers, which separate the planes from each other, see Fig.1a. The nearly squared CuO_2 plane with a Cu $3d_{x^2-y^2}$ orbital bonding to four O $2p_\sigma$ orbitals is present in all cuprates while the charge reservoir composition varies significantly. In Fig.1b the crystal structure of $HgBa_2CuO_{4+\delta}$ is shown as an example with $BaHgO_\delta$ being a charge reservoir layer. The antiferromagnetic parent compounds can be doped with holes or electrons by modification of the chemical composition of the charge reservoir layers and magnetic order vanishes. New electronic phenomena emerge and the systems become conducting or superconducting (see phase diagram in Fig.2a). There are many similarities between different cuprate families, and one typically differentiates only between the hole and electron doped phase diagrams, which show a distinct asymmetry, Fig.2a. However, the extent in temperature and doping of the different phases and observed phenomena vary substantially between different families, also for the much more thoroughly investigated

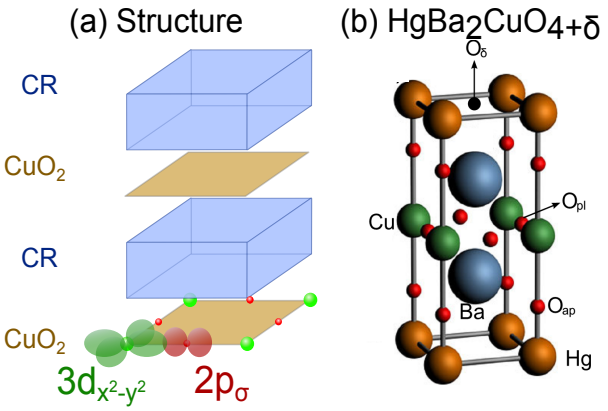

Rys. 1: [From O2] a) Schematic crystal structure of the cuprates consists of two types of building blocks, CuO_2 planes and charge reservoir (CR) layers, the bonding orbitals in the CuO_2 plane are Cu $3d_{x^2-y^2}$ and O $2p_\sigma$, which share the nominal Cu $3d$ hole of the Cu^{2+}; b) crystal structure of $HgBa_2CuO_{4+\delta}$ in which CR layers contain Ba, apical O, Hg and doped O_δ ions.

hole doped materials. In addition, the comparability between different families is somewhat obstructed with regard to doping. For example, while for $La_{2-x}Sr_xCuO_4$ the doping level can be varied over a large range quite reliably by stoichiometry, the interstitial doping with oxygen (O_δ) as, e.g., in $HgBa_2CuO_{4+\delta}$ leaves uncertainties with regard to the actual doping level. In addition, ionic migration may cause phase separation or other ordering phenomena as in the $YBa_2Cu_3O_{7-\delta}$ systems. Nevertheless, from the understanding of the electronic properties we expect, in particular, the clues as how to increase the superconducting transition temperature (T_c) [5] [2].

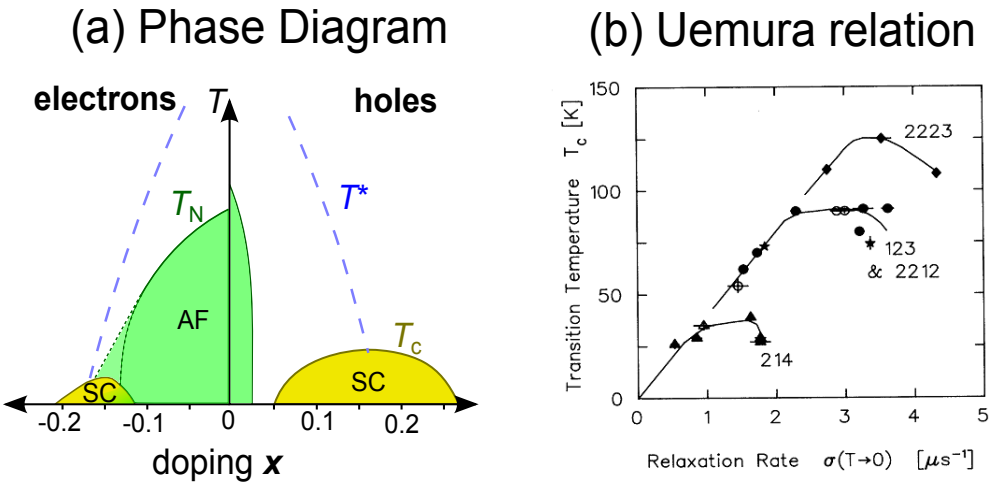

Rys. 2: a) [From O2] Schematic electronic phase diagram of the cuprates for electron (*left*) and hole (*right*) doping x, with antiferromagnetic (AF) and superconducting (SC) phases, T_N and T^* is Neel and pseudogap temperature, respectively. b) Uemura plot, i.e. T_c as a function of muon relaxation rate (σ) extrapolated to T=0 K for $La_{2-x}Sr_xCuO_4$ (214) $YBa_2Cu_3O_{7-\delta}$ (123), two layer and triple layer cuprates containing Bi or Tl (2212, 2223) [1].

The basic parameters given for cuprates are T_c temperature and, inferred from it, the average doping level x of the CuO_2 plane, which is typically read from the phase diagram presented in Fig.2a, especially in the case of cuprates doped by non-stoichiometric O_δ. Taking into account that for the optimal doping level various cuprate families have very different maximal T_c values, one can immediately conclude that the average x is not sufficient for discussing all aspects of the complex properties of the cuprates. Particularly one cannot answer the question

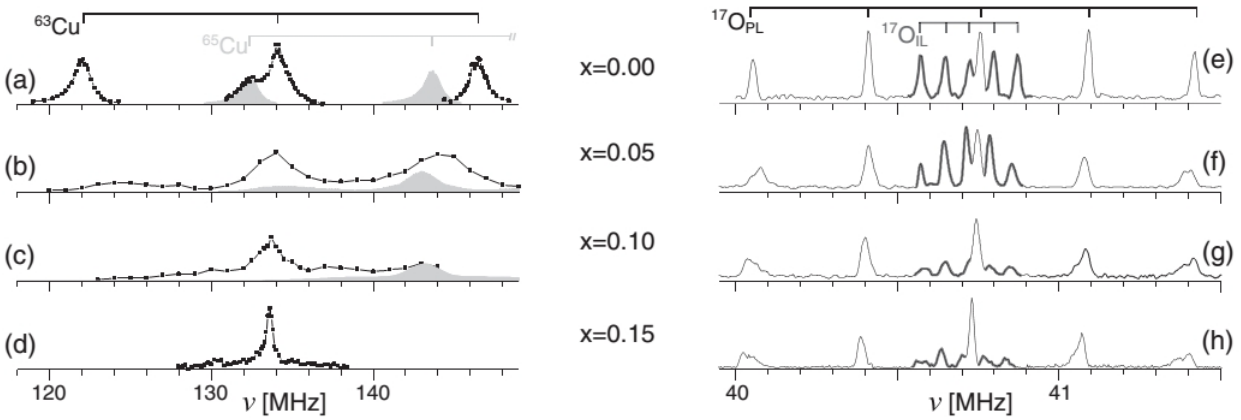

Rys. 3: [From O1] The spectra of $Pr_{2-x}Ce_xCuO_4$ for $c \parallel B_0$ of Cu at 11.74 T [(a)–(d)] and O at 7.05 T [(e)–(h)] for different doping (x). Overlapping ^{65}Cu spectra are indicated in gray in (a)–(c). The spectra of interlayer O are indicated by a thicker line in (e)–(h); the differences in spectral intensities for planar and interlayer (IL) O are due to optimization of excitation conditions for planar (PL) O (selective excitation of the central transition).

why compounds with similar x have so different value of T_c. Researchers looked for other parameters and special attention was given to e.g., distances and shape of the CuO_2 planes, electronic disorder, apical oxygen and magnetic couplings.

Early experimental observations in this regard lead to the famous Uemura plot [1], which is shown in Fig.2b. It shows that the maximum T_c is correlated with the muon spin relaxation rate σ_0 (extrapolated to $T = 0$ K) that is proportional to the superfluid density divided by the effective mass ($\sigma_0 \propto n_s/m^*$). This relation holds for the underdoped materials and orders different cuprate families with respect to their maximum T_c. The Uemura relation and subsequent scaling laws have remained stimulating up to now, and some have shown to be valid for all superconductors [2, 3].

Till now there are only a few such relations, which describe all cuprate families. We recently showed another universal relation, namely how T_c depends on the quadrupole splitting of planar copper and oxygen for all cuprate families [4, 5][O1, O2]. Nuclear electric quadrupole moment for nuclei with spin $I > 1/2$ ($I = 3/2$ for ^{63,65}Cu, $I = 5/2$ for ^{17}O) interacts with the local electric field gradient (EFG) causing a quadrupole splitting (ν_Q) of the NMR lines in high magnetic fields. The EFG at the nuclear site is very sensitive to the local charge symmetry. While NMR measurements on Cu nuclei are rather straightforward, measurements on O are very difficult since the materials have to be enriched with ^{17}O, the naturally abundant ^{16}O nucleus has spin $I = 0$ and NMR measurements on it cannot be conducted. Example measurements of ^{17}O and ^{63}Cu spectra enabling calculation of quadrupole splitting are shown in Fig.3 for the electron doped $Pr_{2-x}Ce_xCuO_4$. It is worth mentioning that our measurements on this family were the first ^{17}O NMR on any electron doped cuprates and still remain the only ones. As can be seen the quadrupole splitting for oxygen ($^{17}\nu_Q$) does not change with doping while the quadrupole splitting for copper ($^{17}\nu_Q$) strongly decreases with doping. On the other hand, the doping dependence for hole doped cuprates is quite different, i.e. both $^{17}\nu_Q$ and $^{63}\nu_Q$ increase with doping.

In order to find a more general relations we collected $^{63}\nu_Q$ and $^{17}\nu_Q$ values for all cuprates, as it is shown in Fig.4. For both types of doping different families are located at different positions of these new phase diagrams. However, it is clear that families, which have high maximum T_c have a small quadrupole splitting of Cu ($^{63}\nu_Q$) and a large of oxygen ($^{17}\nu_Q$). Moreover, the dependence of T_c versus $^{17}\nu_Q$ is very similar to results obtained from μSR by Uemura et al. We plot T_c as a function of both experimental parameters derived from NMR and μSR for similar materials and doping, and find a striking correspondence (Fig.5a). This shows that the muon

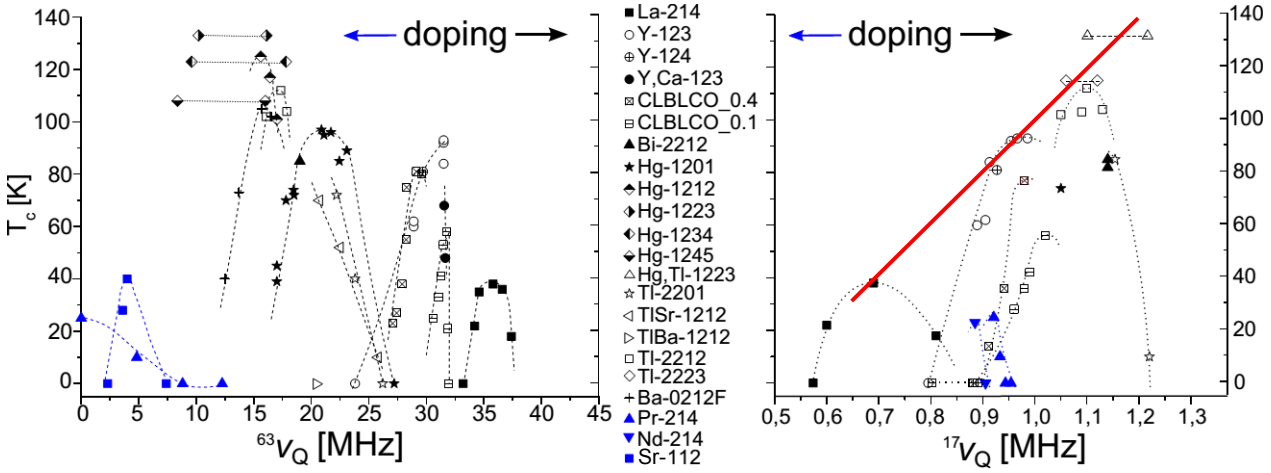

Rys. 4: [From O2] Phase diagrams of cuprates based on quadrupole splittings of the planar copper $^{63}\nu_Q$ (left panel) and oxygen $^{17}\nu_Q$ (right panel). Black and blue symbols and arrows (indicating increase of doping level x) stand for hole and electron doped systems, respectively. Dotted lines are guides to the eye and connect different doping levels for one family. For compounds with three or more CuO_2 layers there are two different planar Cu and O sites, which have different quadrupole splittings, hence the horizontally connected data points belong to the same sample.

spin relaxation rate deep inside the superconducting state is tied to the almost temperature independent EFG at the planar O nuclei, which determines the ^{17}O NMR splitting measured far above T_c, making it an unexpected result. This indicates that the superfluid density is functionally related to the EFG at planar O. Importantly, this correlation suggests that by measuring $^{17}\nu_Q$ even at room temperature one could estimate the maximum achievable value of T_c, which is shown as a red line in Fig.4.

Since the quadrupole splittings of planar Cu and O depend on doping, models have been proposed with attempts to describe these changes in terms of the hole content of certain orbitals, see e.g. Ref.[6]. Based on NMR data on the electron-doped and the parent compounds it was confirmed recently, that NMR quadrupole splittings provide a quantitative measure of the charge distribution in the CuO_2 plane of apparently all cuprates [4][O1]. It was shown that the hole densities in the Cu $3d_{x^2-y^2}$ orbital (n_d) and the O $2p_\sigma$ orbital (n_p) in the CuO_2 plane are related to the experimentally measured splittings $^{63}\nu_Q$ at ^{63}Cu and $^{17}\nu_Q$ at ^{17}O. It is worth mentioning that only after NMR measurements on electron doped families it was realized that parent materials (undoped) of different families, already have different hole contents on oxygen and copper [4][O2].

This finding allowed us to propose a new phase diagram, which includes all families, shown in Fig.5b. It presents the dependence of T_c temperature as a function of the hole content on oxygen ($2n_p$, since there are two oxygen atoms per one of copper) and the hole content on copper (n_d). All cuprates are separated into four groups, shown in different color: (1) $La_{2-x}Sr_xCuO_4$; (2) $YBa_2Cu_3O_{7-\delta}$, and other cuprates with the same crystal structure, e.g., $(Ca_xLa_{1-x})(Ba_{1.75-x}La_{0.25+x})Cu_3O_{6+y}$ and $YBa_2Cu_4O_8$; (3) Bi, Tl and Hg based families; and, finally, (4) the two electron doped systems $Pr_{2-x}Ce_xCuO_4$ and $Nd_{2-x}Ce_xCuO_4$. The parent line, i.e., the line that is given by equation $n_d + 2n_p = 1$ (bold dashed line) separates hole doped and electron doped systems. Note that the lines parallel to the parent line are given by $n_d+2n_p = 1+x$, and thus represent constant hole ($x = +0.1, +0.2$) or electron ($x = -0.1, -0.2$) doping. Interestingly, for the parent compounds we observe that there is a significant variation of hole content on Cu and O, e.g. $2n_p$ varies between 0.15 and 0.45. From the phase diagram it can be concluded that a hypothetical family, which could be promising for higher values of T_c, should have a parent compound with $2n_p$ higher than 0.5.

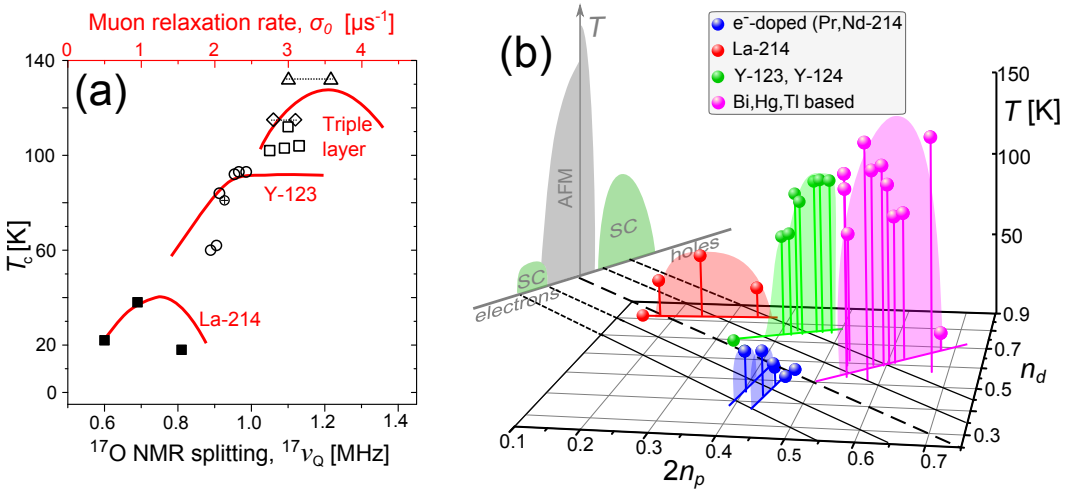

Rys. 5: a)[From O1] The Uemura plot [1], from Fig.2b i.e., T_c vs. muon spin relaxation rate, σ_0 (upper abscissa) with data represented as solid red lines; *black symbols:* T_c vs. planar oxygen quadrupole splitting $^{17}\nu_Q$ for the same materials (lower abscissa). b) T_c as a function of oxygen ($2n_p$) and copper (n_d) hole content for hole doped La-214, Y-123, Y-124, and Bi-, Hg-, Tl-based compounds, as well as electron doped Pr-214 and Nd-214. The parent line (dashed bold black) indicates expectation for the undoped case ($n_d + 2n_p = 1$ from $x = 0$), parallel lines (thin black) correspond to expectation for doping $x = n_d + 2n_p - 1$ changing with a step of 0.1. The commonly used phase diagram (T vs x) is shown as a projection (upper left).

Doping the holes corresponds with entering the right upper half of the $(2n_p, n_d)$-plane. With such a doping both n_d and n_p increase, however, at different rates for different families. As might be expected, if the hole content at oxygen is small, it is easier to add more holes to it rather than to copper. For example La_2CuO_4 has small $2n_p$, but with doping it significantly increases. On the other hand, in Hg family, which has already high oxygen hole content $2n_p$, it is more difficult to add holes to oxygen and more holes go to copper with doping. These changes are shown in the $(2n_p, n_d)$-plane as color solid lines, their different slopes indicate different rate of changes of $2n_p$ and n_d for four different groups in the phase diagram. T_c increases as a function of doping, as well, with a slope that depends on the position on the parent line, as well, and hole doping seems to be more effective in raising T_c. With electron doping we enter the lower left half of the $(2n_p, n_d)$-plane. Here, predominantly Cu holes disappear while the (large) O hole content changes only slightly, i.e. doped electrons go to Cu.

Another important observation concerns the optimal doping, i.e., the doping level for which one finds the highest T_c for a given family. According to our analysis it is related to $x = n_d + 2n_p - 1$ and not to particular values of n_d and n_p. However, we do observe a slight increase of the optimal x with increasing n_p (decreasing n_d). Despite significant structural differences between Hg, Tl, and Bi based cuprates they are located in the same group. Also the number of close CuO_2 layers in multi-layer systems does not result in significant differences in the charge distribution [5][O2]. Note that the doping level x stems from our analysis in terms of n_d and n_p and is not deduced from material chemistry. Our analysis agrees with expectations also for materials doped by interstitial O_δ where doping level x is often derived from the T_c dome [4][O2], so that our phase diagram could be used as an alternative method for estimating the amount of doped charges x.

To summarize, publication [O1] presents results of NMR measurements on $Pr_{2-x}Ce_xCuO_4$ on Cu and O. These measurements helped in theoretical understanding of the relation between quadrupole splittings and hole distribution, particularly in parent materials. Analysis of the literature data already showed interesting observations, however, more detailed understanding and discussion was presented in publication [O2], particularly concerning the correlation

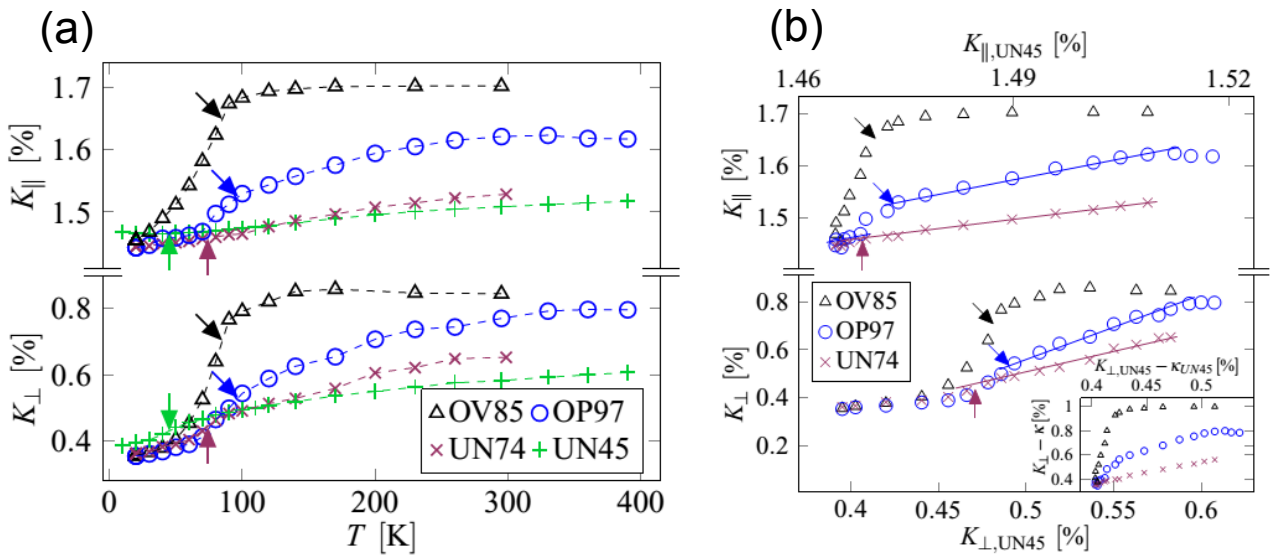

Rys. 6: From [O4]. a) ^{63}Cu shift for $c \parallel B_0$ orientation ($^{63}K_{\parallel}$) and $c \perp B_0$ orientation ($^{63}K_{\perp}$) as a function of temperature for four $HgBa_2CuO_{4+\delta}$ samples: two underdoped with T_c =45 K (UN45) and T_c =74 K (UN74), optimally doped with T_c =97 K (OP97) and overdoped with T_c =85 K (OV85), b) $^{63}K_{\parallel}$ and $^{63}K_{\perp}$ of the UN74, OP97, and OV85 samples plotted vs shift of the UN45 sample with temperature as an implicit parameter. Straight lines have slopes derived from doping ratios (they are not fits).

between the Uemura relation and oxygen quadrupole splitting and its important implications. These studies allowed creating a completely new phase diagram from which one can make much deeper and interesting conclusions compared to standard phase diagram shown in Fig.2a. Particularly one can conclude that the maximum value of T_c increases with the hole content at planar oxygen (n_p), at the expense of the hole content at planar copper (n_d). In other words, a high n_p is a prerequisite for a high maximum T_c and the parent compound must already have a high n_p, which should be further increased by hole doping.

4.3.3 Pseudogap, spin susceptibility and electronic inhomogeneities in the cuprates. [Publications O3-O4-O5]

In cuprates there are other puzzling phenomena. One of them is the pseudogap state observed above T_c in the underdoped region of the phase diagram. Although more than 20 years have passed since the discovery of the pseudogap state, its origin and relation to the superconducting properties are still broadly debated. It was discovered by NMR [7] and its existence was concluded from the temperature dependence of the spin shift. The NMR spin shift, K_s in general can be written as,

$$^{n}K_s(T) = {}^{n}p \cdot \chi_s(T), \tag{1}$$

where ^{n}p denotes the anisotropic hyperfine coupling coefficient for a particular nucleus (n) and χ_s is the spin susceptibility. In a typical metal χ_s is the Pauli spin susceptibility (due to electronic density at the Fermi level) and is temperature independent, but χ_s decreases if metal becomes a spin singlet superconductor. Such a behavior is not observed for underdoped cuprates where the spin shift decreases already at temperatures much higher than T_c (see Fig.6a) and hence a term spin-gap or pseudogap was invoked to explain results of experiments. On the other hand for the overdoped compounds, above T_c, the spin susceptibility is temperature independent (Fig.6a) suggesting Fermi liquid-like behavior, and rapidly decreases below T_c.

Already at the beginning of NMR research on cuprates, scientists raised a question whether one can understand the materials as a single electronic liquid, which would result in a single component of the electronic spin susceptibility. Two early publications, in 1991 [8] and in

1994 [9], reported that such a single-fluid picture is appropriate (while some doubts remained, e.g. from spin-lattice relaxation [10]). However, it was in disagreement with the analysis of normal state uniform susceptibility measurements of $La_{1.85}Sr_{0.15}CuO_4$, which suggested the presence of two components [11, 12]. NMR measurements on this compound also showed that spin shifts could not be explained in terms of a single spin susceptibility as given by Eq. (1).[13] Since one can argue that this could be a peculiarity of the particular system (that has a rather low T_c), we started a study on $HgBa_2CuO_{4+\delta}$ single crystals in the entire doping range these samples can be synthesized. We have found that in this system, the spin shifts cannot be explained in terms of Eq. (1), as well [14, 15] [O3 and O4]. We identified two distinct temperature-dependent spin susceptibilities: one is due to a spin component that is temperature dependent above T_c and reflects pseudogap behavior; the second is Fermi-liquid-like in that it is temperature independent above T_c and vanishes rapidly below T_c. In addition, we demonstrated the existence of a third spin susceptibility, which is temperature independent at higher temperatures, vanishes at lower temperatures and changes sign near optimal doping [15] [O4]. Independent susceptibility measurements on single crystals support its presence in other cuprates as well [16].

Surprisingly, we have also found that the NMR ^{63}Cu shifts of the underdoped and optimally doped $HgBa_2CuO_{4+\delta}$ when plotted against each other with temperature as an implicit parameter, show a linear dependence above T_c (Fig. 6b) with the slope given by the ratio of doped holes, indicating a peculiar scaling of the pseudogap susceptibility [14, 15] [O3 and O4]. Similar scaling was later observed for $YBa_2Cu_4O_8$ from planar ^{17}O NMR shifts, but with doping replaced by pressure, i.e. shifts measured at high pressure plotted against the shift at ambient pressure, show again a linear dependence above T_c [17].

The role of inhomogeneities in the cuprates is still a controversial issue despite long research and discussion (e.g. [18, 19]). In some systems incommensurate charge order has been observed and there is an evidence for strong charge and spin density variations, so-called stripes. Most of the cuprates are not stoichiometric and in general chemical inhomogeneity or order could be expected. This is one of the reasons for the controversy regarding the role of inhomogeneities, which could range from contamination effects (due to chemical doping) to interesting physics causing various types of electronic ordering.

NMR is a powerful local probe, highly sensitive to inhomogeneities or special order (chemical or electronic). There are only two stoichiometric superconducting cuprates ($YBa_2Cu_4O_8$ and $YBa_2Cu_3O_7$) and for them NMR lines are rather narrow, and result from magnetic dipolar interactions (enhanced due to indirect coupling) and electric quadrupolar widths expected for normal strain. On the other hand, doped cuprates have much larger magnetic and electric quadrupolar linewidths. The magnetic linewidths are often temperature dependent, while those due to the electric quadrupole interaction have only a very weak temperature dependence.

We have investigated the NMR linewidths of the optimally doped single crystal of $HgBa_2CuO_{4+\delta}$, in which the dopant resides in the Hg layer and it is far away from the CuO_2 plane. However, our ^{63}Cu NMR data show (Fig. 7) very large quadrupolar linewidth for the two satellite transitions caused by a local variation of the charge density at Cu site [20] [O5]. As was mentioned above, the average quadrupole splitting of the planar copper in hole doped cuprates is a linear function of the local charge (hole) density x. Therefore, it is plausible to assume that the quadrupolar linewidth could be caused by a spatial variation of the local charge density x. One could express the quadrupolar linewidth in terms of a charge density variation and plot the quadrupolar lineshape with the frequency axis converted to a local doping axis, as shown in Fig.7d. The linewidth or the root-mean-square charge density variation is about 0.073 at a nominal average doping of $x = 0.16$. Looking at Fig.7d one notes that the local doping approaches that of the antiferromagnet to the left and that of a strongly overdoped material to the right.

At first it was difficult to convince the scientific community that it is not due to the sam-

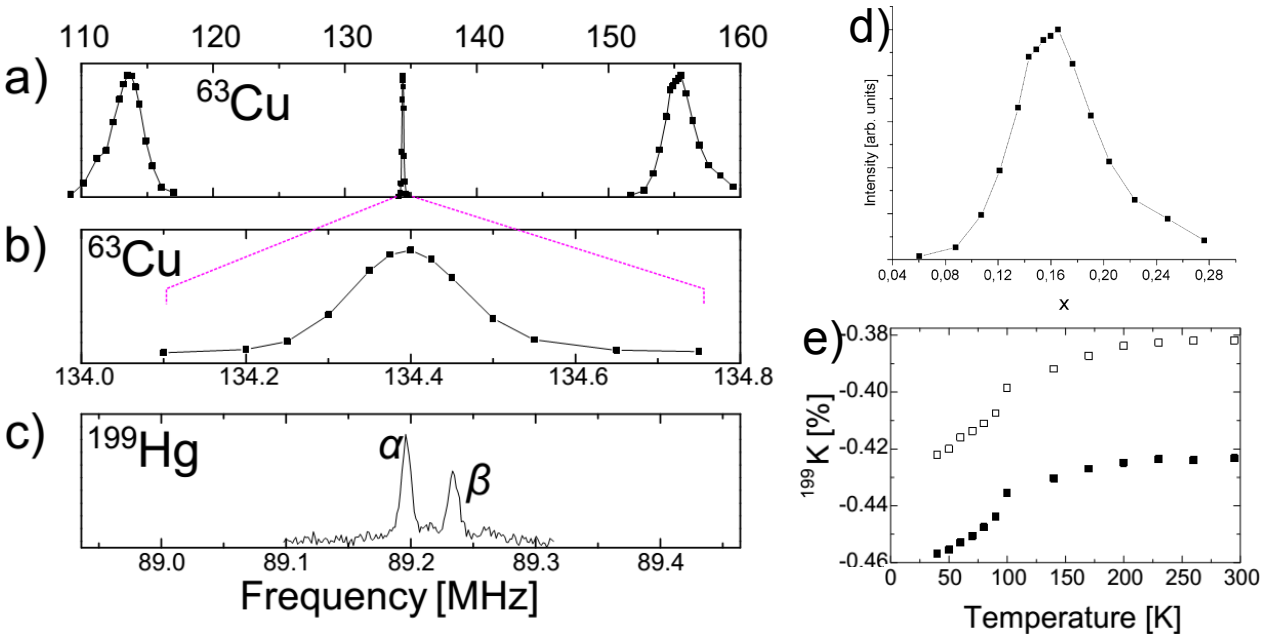

Rys. 7: a) - c) NMR spectra of the optimally doped $HgBa_2CuO_{4+\delta}$ measured at 11.74 T. a) ^{63}Cu spectrum with very broad satellite lines and central line, which is shown in different scale in b) (all lines are normalized to 1). Panel c) shows ^{199}Hg spectrum with two lines due to two Hg lattice sites. In panels b) and c) frequency range is scaled as it would be in a ppm scale (to show very large difference between magnetic linewidths of ^{63}Cu and ^{199}Hg). d) The quadrupolar satellite lineshape plotted against the local hole content x, where the central frequency corresponds to the hole content $x = 0.16$. e) Temperature dependence of shifts ^{199}K for the α (solid squares) and β line (empty squares) [20, 14] [O4 and O5].

ple quality, but is rather related to intrinsic local charge density fluctuations, which are now also seen by X-ray techniques [21]. Over the past, many models of electronic ordering have been proposed including stripe order that combines spatial spin and charge density variations. NMR measurements on underdoped $YBa_2Cu_3O_y$ appear to show an onset of static charge ordering only at high fields [22, 23], while X-ray studies indicate the presence of a fluctuating incommensurate charge density wave (CDW) order at zero field. This fluctuating CDW order has a rather small correlation length (20 lattice constants in-plane and 1 lattice constant out-of-plane) and appears in the pseudogap phase above T_c [24, 25, 26, 27, 28]. Recent X-ray scattering experiments carried out by M. Greven's group suggest that such an order exists in underdoped $HgBa_2CuO_{4+\delta}$ (T_c=74 K) below 200 K. However, the reported correlation length is much smaller (seven lattice constants) [21]. Similar charge modulations have also been observed in optimally doped $Bi_{1.5}Pb_{0.6}Sr_{1.54}CaCu_2O_{8+\delta}$ [29]. It is currently not clear whether NMR and X-ray studies see the same type of charge modulations.

The conclusion that the large quadrupolar linewidths seen by ^{63}Cu NMR is not due to simple chemical inhomogeneities is supported by ^{199}Hg (nuclear spin $I = 1/2$) NMR that shows two very well resolved Hg lines (Fig. 7c). We observed two Hg lines due to the fact that samples are not stoichiometric, i.e. due to possible presence of O_δ in the Hg plane (Fig.1b). One Hg site (α) has no O_δ as the nearest neighbor and the other Hg site (β) has one O_δ as the neighbor. Sites with more O_δ neighbors are also possible, but their probability and corresponding NMR signal intensities are too low to be observable (δ is smaller than 0.1). Linewidths of Hg are much smaller compared with Cu, which indicates that Hg is much less affected by the charge density variations present in the CuO_2 plane, and the two lines prove that the chemical structure does not vary spatially for both sites (α and β). It is still not clear what the location of O_δ defect in $HgBa_2CuO_{4+\delta}$ is. Early diffraction studies suggested that doped oxygen is located in the center of a square consisting of four Hg ions as shown in Fig.1b. However, a study by Jorgensen et

al. suggested that this O site is predominantly occupied only in the overdoped samples while in the underdoped oxygen moves to another position in the Hg plane [30]. The knowledge of the position of O_δ is important since it could, e.g., lead to different properties of CuO_2 plane, as discussed recently [31]. With two Hg lines resolved one could study the local structure of $HgBa_2CuO_{4+\delta}$, e.g., the position of O_δ in the HgO_δ layer or Hg deficiency [32]. This, however, remains to be investigated.

Research on $HgBa_2CuO_{4+\delta}$ family resulted in finding that the spin suspceptibility does not have only one component, as assumed before, but at least two. It is important for interpretation of other magnetic measurements in studied materials and also in other cuprates since $HgBa_2CuO_{4+\delta}$ family is considered a model compound due to simple crystal structure. Second important aspect is the electronic homogeneity, particularly in terms of the charge density distribution. It was shown that there is a large charge (hole) density distribution in the copper-oxygen plane, which is now observed also in other cuprates by different techniques. However, the HgO_δ plane appears to be not affected by these electronic density variations. It is worth mentioning that the observation of the two ^{199}Hg lines was made possible only with the single crystals.

4.3.4 Electronic phase separation or correlated spin/charge density variations in $CeFeAsO_{0.8}F_{0.2}$ iron pnictide. [Publication O6]

Iron pnictides are a new family of high temperature superconductors with the second highest (at ambient pressure) superconducting transition temperatures after the cuprates. They have attracted a considerable attention because of the complex Fermi surface and similarities to the cuprates (e.g. the parent compounds display magnetic order, which is suppressed by the doping). We studied a compound from so called 1111 family, i.e. $CeFeAsO_{0.8}F_{0.2}$, an overdoped superconductor with T_c =20 K and carried out temperature and field dependent ^{75}As NMR shift and spin-lattice relaxation time (T_1) measurements.

Fig.8a shows ^{75}As central transition line at different temperatures. At higher temperatures one can see a single line, which gradually shifts to higher frequencies and at low temperatures another line appears. The obtained NMR shifts are presented in Fig.8b and they show a Curie-Weiss like dependence, which is attributed to a hyperfine coupling of the Ce magnetic moments to ^{75}As. Presence of such coupling is also concluded from a temperature dependence of spin-lattice relaxation rates, which also suggest that the mechanism of relaxation is due to 2D antiferromagnetic spin fluctuations. Previous specific heat measurements suggested that Ce moments order antiferromagnetically below 1.8 K [33].

However, the most interesting result concerns the origin of two ^{75}As central lines. For similar compound $CeFeAsO_{0.84}F_{0.16}$ two lines were also observed, but only below T_c and were attributed to signals from regions inside and outside of the vortices present in the mixed state [34]. In our measurements, which were conducted at higher fields, two lines appear also above T_c. Additionally, our field dependent measurements indicated that the interpretation of *Ghoshray et al.* was not correct. In Fig.8c we show a ^{75}As spectrum measured at 10 K consisting of four lines in total (including central and satellite lines). With two central lines and a non zero quadrupole splitting there should be four satellite lines appearing in the spectrum (one central and two satellites for each As local environment, since ^{75}As has a nuclear spin $I = 3/2$). However, this is not what is observed and lines α and β must therefore be a convolution of two satellites. Different linewidths of lines α and β can be explained by assuming that As ions from the upper and lower central line have different quadrupole splitting, $\nu_{sat2} = \nu_{c2} \pm \nu_{q2}$ and $\nu_{sat1} = \nu_{c1} \pm \nu_{q1}$, and the result is sketched in Fig.8c. There are two possible explanations of our observations. The first is a phase segregation into regions with two different electronic doping levels. The second is a correlated spatial charge and spin density variations. In such a picture charge density variations are responsible for two different quadrupole couplings, while

the spin density variations result in a different temperature dependence of the NMR shifts. Such correlated variations have been observed in doped cuprates, e.g. in $La_{2-x}Sr_xCuO_4$ [35].

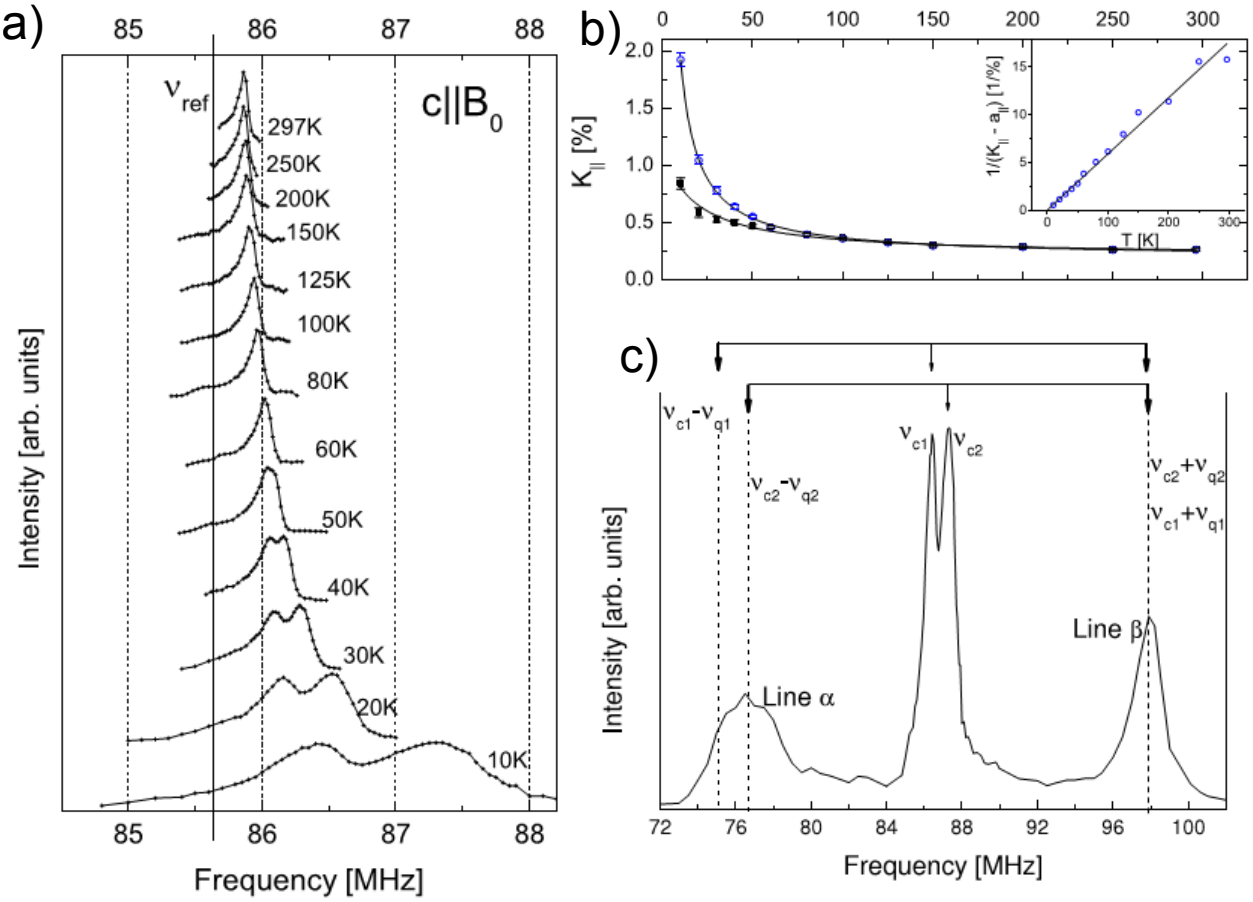

Rys. 8: From [O6] a) Temperature dependence of ^{75}As central transition line of $CeFeAsO_{0.8}F_{0.2}$ for $c \parallel B_0$ measured at 11.75 T where ν_{ref} is the reference frequency. b) Temperature dependence of shifts $^{75}K_{\parallel}$ for both lines, the inset shows $1/(K_{\parallel} - a_{\parallel})$ with $a_{\parallel} = 0.2\%$ versus temperature for the upper line. Solid lines are fits to the data. c) ^{75}As spectrum showing central and satellite transition lines at 10 K for $c \parallel B_0$. Lines on top show signal assignment to As ions with different local environment (different NMR shift and quadrupole splitting), ν_{c1} and ν_{c2} are frequencies of the lower and upper central line, respectively, ν_{q1} and ν_{q2} are corresponding quadrupole splittings.

4.3.5 Electronic properties of manganites studied by NMR and synchrotron radiation. [Publications O7 and O8]

Mixed-valent manganese perovskites show a plethora of types of magnetic, charge, and orbital orders, which occur due to interplay of various degrees of freedom including spin, charge, and the lattice. Adding chemical doping, temperature, or external pressure as parameters leads to even more complicated phase diagrams, but it also allows for tuning their properties to those required for given applications, e.g., in spintronics, catalysis, or solar energy-to-fuel conversion.

They are also studied due to their colossal magnetoresistance (CMR) properties, which occur by application of magnetic field. We studied this effect in electron doped $Sm_{0.55}Sr_{0.45}MnO_3$ by means of ^{55}Mn NMR, which is the first NMR study of this family of manganites. $Sm_{0.55}Sr_{0.45}MnO_3$ has a Curie temperature (T_{Curie}) of about 125 K and is ferromagnetic metallic (FMM) below it, and charge ordered and insulating above it. In magnetic materials NMR measurements are also possible without external magnetic field since at nuclei there is already magnetic field present due to the magnetic order. This is called effective field, B_e and can be calculated from the

relation $\gamma \cdot B_e = 2\pi \cdot \nu$, where γ is the gyromagnetic ratio and ν is the resonance frequency.

Below T_{Curie} we observed a single resonance line, which is due to the double-exchange (DE) interaction between Mn^{3+} and Mn^{4+} ions [36], which results in ferromagnetic order of Mn moments and metallic properties of the material. However, in manganites this DE line has also been observed above T_{Curie}, i.e. in the paramagnetic state with no long range order [37]. It is attributed to presence of small, micrometer in size, ferromagnetic metallic (FMM) clusters in a paramagnetic and insulating matrix. We find that B_e is only weakly temperature dependent and does not vanish at T_{Curie} similarly to other manganites. It decreases merely by 11% between 4.2 K and 139 K (see Fig.9 for the temperature range between 95 K and 135 K), which indicates almost fully saturated Mn magnetization in the FMM regions in this temperature range. This also shows that the magnetic transition is of first order, in agreement with resistivity measurements.

In order to investigate the CMR behaviour also magnetization measurements at 0.01 T, 1 T and 2 T were carried out. The results are shown in Fig.9 together with the temperature dependence of the intensity of the DE line measured at zero field. The plots show that the profile of the temperature dependent NMR intensity is very similar to that of the magnetization data obtained at a small field of 0.01 T. Since the intensity of the DE line is proportional to the number of ^{55}Mn nuclei in FMM clusters, the decrease of NMR intensity indicates that the content of the FMM phase decreases with temperature increase. At 139 K (i.e. above T_{Curie}), application of a field of 1 T enhances the intensity of the DE line considerably. It becomes at least thirty times larger than that at zero field state, and at 2 T the increase is even larger. Therefore, we conclude that application of magnetic field increases either the number of these clusters or their volume, both effects leading to a percolation of FMM regions. Moreover, we observed that application of magnetic field resulted in a change of the resonance frequency, which indicated an antiferromagnetic coupling of FMM clusters.

Our observations revealed that metallicity is induced in $Sm_{0.55}Sr_{0.45}MnO_3$ by the applied magnetic field and explained the CMR effect at the microscopic level. Our conclusions agree with previous results, which confirms that the percolation of the FMM clusters is responsible for the CMR effect.

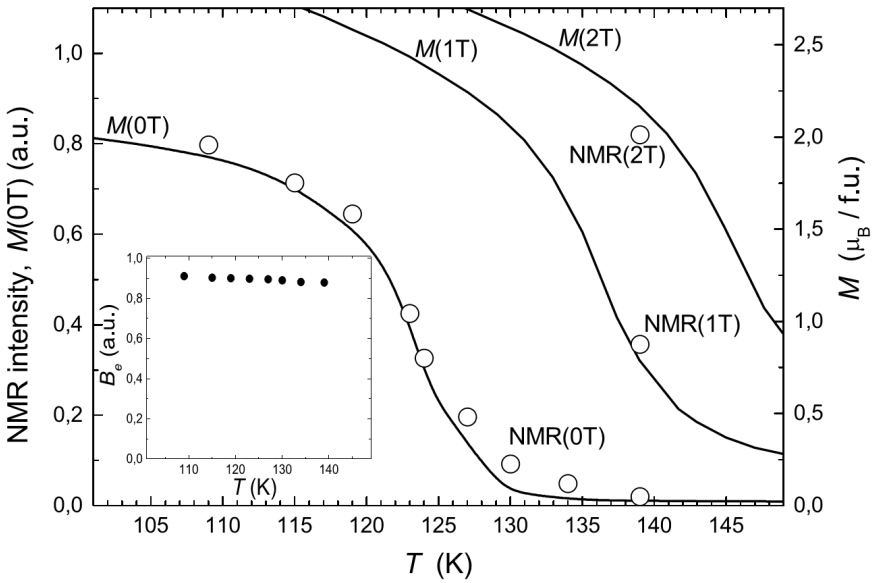

Rys. 9: From [O7] Temperature dependence of the magnetization M (solid lines), the intensity of the DE NMR line (open circles) and the effective magnetic field B_e normalized at 4.2 K (in the inset).

X-ray absorption and emission spectroscopy (XAS and XES, respectively) is sensitive to

the local structure, spin, and charge and has been used to study the interplay between the local crystal structure and the electronic properties in manganites for about 20 years. However, owing to the recent advances in high-resolution hard x-ray photon-in photon-out spectroscopy [38], background-free XAS and valence-band XES can be probed giving access to even more details on the hybridization and evolution of electronic bands near the Fermi level. Therefore, we used this technique to study bilayered perovskites, i.e. $La_{2-2x}Sr_{1+2x}Mn_2O_7$ family (for $0.5 \leq x \leq 1$), which has not been studied by XAS/XES before. This is an interesting family due to relatively small lattice distortions, compared to pseudo-cubic $La_{1-x}Sr_xMnO_3$ or single-layer $La_{1-x}Sr_{1+x}MnO_4$, and the fact that samples can be synthesized only starting from $x \geq 0.3$.

In the absorption spectra the pre-edge region shows a behavior typical for mixed-valent manganites, i.e. with doping the pre-edge centroid shifted to higher energy and the total intensity of the pre-edge area increased. We showed that the most intense feature in the pre-edge is mostly of nonlocal dipolar origin, i.e. it results from transition from $1s$ to $3d$ states of neighboring metal sites through the oxygen-mediated intersite hybridization Mn($4p$)-O($2p$)-Mn'($3d$). The intensity of this feature was increasing with doping and we showed that it follows the probability of all neighbors of the absorbing Mn ion being Mn^{4+}. Since Mn^{4+} ions have more empty states available on orbitals of the e_g symmetry (σ-like) compared to Mn^{3+}, more Mn^{4+} ions as neighbors should make Mn($4p$)-O($2p$)-Mn'($3d$) hybridized states more probable. The main absorption edge was also shifting (linearly) to higher energies with increasing doping. The extrapolation of this linear trend to x=0,. i.e. to a hypothetical $La_2SrMn_2O_7$ gives the edge energy higher by approx. 1 eV compared to $LaMnO_3$ (both compounds contain formal Mn^{3+} ions), see Fig.10a.

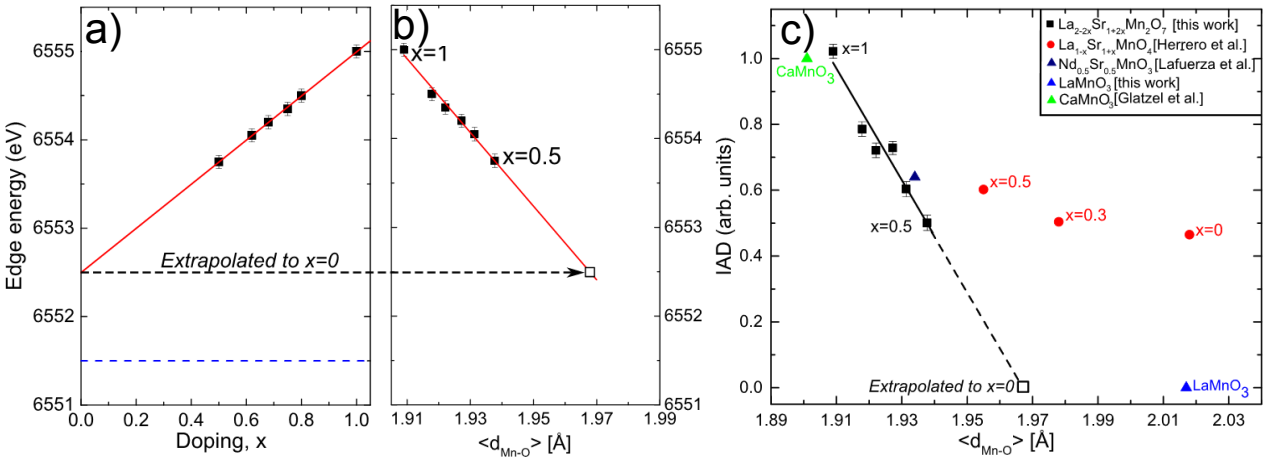

Rys. 10: From [O8] The edge energy of $La_{2-2x}Sr_{1+2x}Mn_2O_7$ as a function of a) doping x and b) average Mn-O distance $< d_{\mathrm{Mn-O}} >$. Dashed blue line shows the edge energy for $LaMnO_3$, solid red lines are linear fits. Empty black square is the value extrapolated to $La_2SrMn_2O_7$ (x=0). c) Normalized IAD for $La_{2-2x}Sr_{1+2x}Mn_2O_7$, $La_{1-x}Sr_{1+x}MnO_4$ [39], $Nd_{0.5}Sr_{0.5}MnO_3$ [40] with respect to $LaMnO_3$ (IAD=0) and $CaMnO_3$ (IAD=1) [41, 38]. Solid black line is a linear fit to data for $La_{2-2x}Sr_{1+2x}Mn_2O_7$ samples.

X-ray emission spectra covered both core-to-core (CTC) transitions corresponding to $K\beta_{1,3}$ main line and $K\beta'$ satellite as well as the valence-to-core (VTC) transitions corresponding to $K\beta_{2,5}$ and Kβ'' features. Here only CTC lines are discussed, which, due to strong spin selectivity, are sensitive to the net spin $3d$ moment [42]. In order to perform quantitative analysis of the CTC spectra, we used the method of integrated absolute difference (IAD) [43]. We found that IAD depends linearly on doping (formal Mn valence). The change of IAD between x=1 and x=0.5 samples was roughly half of that between $CaMnO_3$ and $LaMnO_3$ indicating that doping affects mostly charge on Mn ions. Such an IAD dependence on Mn formal valence was observed in some Mn oxides or undoped manganites (e.g $LaMnO_3$ and $CaMnO_3$) [38]. However, it is

different from the behavior observed for single-layer $La_{1-x}Sr_{1+x}MnO_4$, where almost identical IAD values are observed in the broad doping range [39], which was attributed to localization of doped charge on apical oxygen rather than on Mn.

We found that XANES and XES parameters, which depend on the local structure, showed such a doping dependence that their extrapolation to a hypothetical $La_2SrMn_2O_7$ (x=0) would result in significantly different values than that observed for $LaMnO_3$. At the first sight one might think that this is obviously due to the fact that $LaMnO_3$ has very different type of crystal and local structure (distortion of MnO_6 octahedra). However, the single layer $LaSrMnO_4$ has a tetragonal structure as bilayered compounds have, but its edge energy is nearly the same as for $LaMnO_3$ [44]. From the dependence of the edge energy and IAD plotted as a function of $< d_{\mathrm{Mn-O}} >$, one can estimate the expected average Mn-O distance for x=0 bilayered compound. Extrapolations shown in Fig.10 indicate $< d_{\mathrm{Mn-O}} > \approx 1.97(1)$ Å. However, a structure with such small $< d_{\mathrm{Mn-O}} >$ is unlikely to be realized, taking into account ionic radii of six-fold coordinated formally Mn^{3+} (0.645 Å) and two-fold coordinated O^{2-} (1.35 Å). On the other hand, single-layer $La_{1-x}Sr_{1+x}MnO_4$ can be synthesized from x=0, but such a compound has the structure strongly elongated along c-axis resulting in very strong distortion and $< d_{\mathrm{Mn-O}} >$ of about 2.02 Å, which is nearly identical to that in $LaMnO_3$. The main difference between these systems is related to structural anisotropy. In single-layer compounds the distortion of MnO_6 octahedra is static, while in the pseudocubic manganites the dynamic Jahn-Teller effect is present. Upon comparison of IAD between these families and bilayered one, characterized by non-distorted octahedra, we can deduce that the local charge transfer from Mn towards oxygen is enhanced by static distortion. Provided that lattice can accommodate such a distortion (anisotropic charge distribution), the compound might be stable. Apparently, it is not the case of bilayered family, where simultaneous distortion and charge transfer are not possible in the rigid crystal structure.

Our observations indicate that there is an intimate relation between the $< d_{\mathrm{Mn-O}} >$ and the localized Mn charge, which enables a formation of stable structures. We explained why $La_{2-2x}Sr_{1+2x}Mn_2O_7$ family cannot by synthesized in the entire doping range. Additionally, we proposed that our analysis could be applied to other transition metal oxide families in order to assist in prediction of their structural stability upon e.g. chemical doping or external pressure.

4.4 Summary

An important progress has been made in understanding the superconducting cuprates, especially in defining material parameters responsible for setting the T_c values. The key feature appears to be the distribution of charge between Cu and O in the copper-oxygen plane. In order to increase T_c one has to increase the hole content at oxygen at the expense of copper. Discovery of new cuprate family with such charge transfer could lead to increase of T_c, which has not been raised for the past 20 years. It should be stressed that results and analysis of own NMR measurements were used to find a relation valid for all cuprates, and to suggest how to increase T_c. There are only a few such general relations known. The second finding is related to the electronic spin susceptibility, which has been interpreted as having only one component. NMR studies on $HgBa_2CuO_{4+\delta}$ showed that such interpretation was not correct. Another result of studies on $HgBa_2CuO_{4+\delta}$ concerns the charge homogeneity. It was observed that even in high quality single crystals there is a large distribution of charge density in the copper-oxygen plane indicating significant spatial fluctuations of hole content at copper and oxygen. It was also found that correlated spin and charge density fluctuations could also be present in a superconductor from the iron pnictide group, i.e. $CeFeAsO_{0.8}F_{0.2}$.

Phase separation, and more precisely, the existence of ferromagnetic metallic clusters in paramagnetic matrix was found to be responsible for the colossal magnetoresistance effect in manganese perovskite $Sm_{0.55}Sr_{0.45}MnO_3$, as it was concluded from NMR measurements at

the applied magnetic field. Investigation of bilayered manganites, $La_{2-2x}Sr_{1+2x}Mn_2O_7$ using synchrotron radiation methods allowed to study the evolution of spin and charge on Mn and to correlate these changes with changes of the local crystal structure. Our conclusions also indicated why this family cannot be synthesized in the entire doping range.

It is worth mentioning that in my research I did not focus only on one group of materials, but I also studied recently discovered iron pnictides and manganese perovskites. In my research work I carried out NMR measurements on many isotopes including ^{17}O, ^{27}Al, ^{55}Mn, ^{57}Fe, ^{59}Co, ^{63,65}Cu, ^{69,71}Ga, ^{77}Se, ^{97}As, ^{139}La and ^{199}Hg. Additionally, for magnetic materials I was using other methods, partly complementary to NMR, exploiting synchrotron radiation in order to study changes of charge and spin density.

4.5 Future plans

A few days before I wrote these words it has been announced that a new cuprate family Ga-Ba-Ca-Cu-O with T_c of 116 K has been discovered, [45]. Clearly there is still a room for research and important discoveries in the cuprates. Therefore, I would like to continue my studies on high-temperature superconductors, particularly with the aim to study the problem of charge distribution in the copper oxygen plane. This applies to $HgBa_2CuO_{4+\delta}$ family, for which the analysis is not finished at the moment. Additionally, our ^{199}Hg NMR measurements suggest that that there is a change of the local structure in the HgO_δ upon doping, but it requires further investigation on samples with different dopings. This will be done in collaboration with Prof. J. Haase from Leipzig University and Prof. M. Greven from Minnesota University. However, I do not want to limit myself to one family of cuprates and I already established a collaboration with dr. Z. Bukowski from Institute of Low Temperatures (Wroclaw) regarding preparation of compounds from different family. We also plan to use synchrotron methods to compare results with NMR (in collaboration with dr. hab. M. Sikora from AGH in Krakow).

5 Discussion of other scientific activities

I become interested in NMR technique already during my master's studies and I continued using this method also for my PhD degree, which I obtained for NMR studies on manganese perovskites. My PhD studies were a part of the SCOOTMO Research Training Network and I actively participated in international exchanges, workshops and meetings. I obtained the PhD degree from AGH University of Science and Technology (Krakow, Poland) and Charles University (Prague, Czech Republic) with a honorable mention. Additionally, for a couple of months I stayed at the Institute of Physics of Czech Academy of Sciences in Prague in the group of Dr. Z. Jirak, where I learned how to prepare samples using the solid state reaction method, I successfully prepared pseudo-cubic manganites from the $La_{1-x}Na_xMnO_3$ family.

However, NMR was not the only technique I got acquainted with during my studies. I am also familiar with techniques using synchrotron radiation. My first contact with synchrotron methods was during my master's studies when I participated in Summer Student Program in DESY Hamburg. During this stay I was involved in statistical data analysis in the ABLO experiment in the Free Electron Laser. While conducting my NMR studies I also took part in several measurement sessions utilizing synchrotron radiation in Hasylab, Hamburg and in ESRF, Grenoble. I learned several techniques including x-ray absorption (XAS), x-ray circular magnetic dichroism (XMCD), extended x-ray absorption fine structure (EXAFS) and x-ray absorption near edge spectroscopy (XANES). These studies concerned mostly manganese perovskites from several different families. Predominantly, we were interested in changes of the electronic properties as a function of different dopants and/or dopant concentration. The results of this research were published e.g. in *Physical Review B, Applied Physics Letters, Journal of Magnetism and Magnetic Materials*. During that time I also participated, for the first time, in

research on systems with reduced dimensionality (nanoparticles) of magnetic compounds (manganese perovskites and surface oxidized iron particles) and I conducted NMR measurements on ^{55}Mn and ^{57}Fe in these materials.

After obtaining my PhD degree I started my 7 year long post-doctoral stay at Leipzig University in the group of Prof. J. Haase. During first two years my employment was a part of the COMEPHS Research Training Network and again I had the opportunity to vividly collaborate with many leading researchers from Europe. For the remaining five years I had an university funded position, which required some teaching work from me (2 hours per week). My main research area there was NMR on superconductors, which were new materials for me and I mostly studied $HgBa_2CuO_{4+\delta}$ family, as was discussed above. During my stay in Leipzig I also spent one month in the Industrial Research Limited in Wellington, New Zealand, in the group of Prof. G. V. M. Williams where I was working on preparation of electron doped cuprates from $Pr_{2-x}Ce_xCuO_4$ family. Samples prepared by me were later measured with NMR by E. Veroutis (with my training and assistance), who obtained the Master's degree for the thesis based on these measurements. I also closely collaborated with M. Jurkutat on his Master's thesis who also was investigating electron doped cuprates with NMR. Part of results on oriented powder samples with Cu substituted by Ni, which induced a spin density oscillation, were published in *Journal of Physics: Condensed Matter*. Later, owing to the collaboration with Prof. A. Erb, we measured single crystal samples, which allowed us to obtain much more detailed information and directly lead to publication O1.

In Leipzig I also had the opportunity to take part in a groundbreaking research on high pressure NMR. Group of Prof. J. Haase with collaboration with Prof. P. Littlewood and Dr. S. K. Goh from Cavendish Laboratory (Cambridge University) developed a new high pressure anvil cell for NMR, which could achieve GPa pressure range. This is very difficult task since a NMR microcoil had to to placed in a high pressure region between the anvils. Moreover, the pressurized region is microliter in volume and the samples are extremely small, which makes measurements very difficult also due to relatively small NMR sensitivity. Before the developments done in Leipzig the detection coil for NMR was usually placed around the entire pressure cell, which means that the sample was only a very small fraction of the detection coil volume. Placing coil between the anvils i.e. directly around the sample tremendously increased the signal-to-noise-ratio, which made NMR measurements possible. I participated in these developments, which resulted in two publications, one in *Review of Scientific Instruments* and the second in *Journal of Low Temperature Physics*. Soon after, a similar set-up was developed at the Tokyo University. Now more groups are actively pursuing, since high pressure research has become very topical recently, partly due to record high superconducting transition temperature discovered in hydrogen sulfide at extremely high pressures. I started high pressure NMR measurements on the optimally doped $HgBa_2CuO_{4+\delta}$ sample. Unfortunately, due to technical problems I could not complete the measurements and publish results. Nevertheless, I showed that such measurements are feasible in doped superconductors, which have broad NMR lines (prior NMR measurements were done on samples, which showed lines with significantly smaller widths).

In the meantime I was also involved in research on topological insulators, which became a hot topic recently. I helped N. Georgieva, whom I trained with NMR technique, in studies of Bi_2Se_3 (doped with Cu) single crystals by means of ^{77}Se NMR. First, we found two resonance lines and showed that they originate from the two inequivalent Se lattice sites and not from topological states as claimed before from measurements on powder samples. Second, we observed unusual field-independent linewidths and attributed them to an unexpectedly strong internuclear coupling mediated by bulk electrons. The results were published in *Physical Review B* and are part of the PhD thesis of N. Georgieva.

After returning to Poland I have been continuing my research on superconductors and magnetic compounds. I am now a PhD co-supervisor of T. Strączek, who is studies super-

paramagnetic nanoparticles for biomedical applications by means of Mossbauer spectroscopy, magnetic susceptibility and magnetization measurements as a function of temperature and magnetic field.

References

[1] Y. J. Uemura et al. In: *Phys. Rev. Lett.* 62 (1989), p. 2317.
[2] C. C. Homes et al. In: *Nature* 430 (2004), p. 539.
[3] S. V. Dordevic, D. N. Basov, and C. C. Homes. In: *Sci. Rep.* 3 (2013), p. 1713.
[4] M. Jurkutat et al. In: *Phys. Rev. B* 90 (2014), p. 140504.
[5] D. Rybicki et al. In: *Nature Commun.* 7 (2016), p. 11413.
[6] J. Haase et al. In: *Phys. Rev. B* 69 (2004), p. 0945041.
[7] H. Alloul, T. Ohno, and P. Mendels. In: *Phys. Rev. Lett.* 63 (1989), p. 1700.
[8] M. Takigawa et al. In: *Phys. Rev. B* 43 (1991), p. 247.
[9] M. Bankay et al. In: *Phys. Rev. B* 50 (1994), p. 6416.
[10] R. E. Walstedt, B. S. Shastry, and S-W. Cheong. In: *Phys. Rev. Lett.* 72 (1994), p. 3610.
[11] D. C. Johnston. In: *Phys. Rev. Lett.* 62 (1989), p. 957.
[12] T. Nakano et al. In: *Phys. Rev. B* 49 (1994), p. 16000.
[13] J. Haase, C. P. Slichter, and G. V. M. Williams. In: *J. Phys. Condens. Matter* 21 (2009), p. 455702.
[14] J. Haase et al. In: *Phys. Rev. B* 85 (2012), p. 104517.
[15] D. Rybicki et al. In: *Phys. Rev. B* 92 (2015), p. 081115.
[16] I. Kokanović, J. R. Cooper, and Kazumasa Iida. In: *EPL* 98 (2012), p. 57011.
[17] T. Meissner et al. In: *Phys. Rev. B* 83 (2011), p. 220517.
[18] J. Haase et al. In: *J. Supercond.* 13 (2000), p. 723.
[19] P. M. Singer, A. W. Hunt, and T. Imai. In: *Phys. Rev. Lett.* 88 (2002), p. 047602.
[20] D. Rybicki et al. In: *J. Supercond. Nov. Magn.* 22 (2009), p. 179.
[21] W. Tabis et al. In: *Nature Commun.* 5 (2014), p. 5875.
[22] T. Wu et al. In: *Nature* 477 (2011), p. 191.
[23] T. Wu et al. In: *Nat. Commun.* 4 (2013).
[24] J. Chang et al. In: *Nat. Phys.* 8 (2012), p. 871.
[25] G. Ghiringhelli et al. In: *Science* 337 (2012), p. 821.
[26] A. J. Achkar et al. In: *Phys. Rev. Lett.* 109 (2012), p. 167001.
[27] S. Blanco-Canosa et al. In: *Phys. Rev. Lett.* 110 (2013), p. 187001.
[28] E. Blackburn et al. In: *Phys. Rev. Lett.* 110 (2013), p. 137004.
[29] M. Hashimoto et al. In: *arXiv:1403.0061* (2014).
[30] J. D. Jorgensen et al. In: *Physica C* 282-287 (1997), p. 97.
[31] Jia-Wei Mei, Alexey A. Soluyanov, and T. M. Rice. In: *Phys. Rev. B* 89 (2014), p. 161115.
[32] E. V. Antipov, A. M. Abakumov, and S. N. Putilin. In: *Supercond. Sci. Tech.* 15 (2002), R31.
[33] G. F. Chen et al. In: *Phys. Rev. Lett.* 100 (2008), p. 247002.
[34] A. Ghoshray et al. In: *Phys. Rev. B* 79 (2009), p. 144512.
[35] J. Haase, C.P. Slichter, and C.T. Milling. In: *J. Supercond.* 15 (2002), p. 339.
[36] G. Matsumoto. In: *J. Phys. Soc. Jpn.* 29 (1970), pp. 615–622.
[37] Cz Kapusta et al. In: *J. Phys.: Cond. Matter* 11 (1999), p. 4079.
[38] P. Glatzel et al. In: *J. Electron Spectr. Rel. Phenom.* 188 (2013), pp. 17–25.
[39] J. Herrero-Martín et al. In: *Phys. Rev. B* 82 (2010), p. 075112.
[40] S. Lafuerza et al. In: *Phys. Rev. B* 93 (2016), p. 205108.
[41] J. Blasco et al. In: *Phys. Rev. B* 62 (2000), pp. 5609–5618.
[42] P. Glatzel and U. Bergmann. In: *Coord. Chem. Rev.* 249 (2005), pp. 65–95.

[43] J. P. Rueff et al. In: *Phys. Rev. B* 63 (2001), p. 132409.
[44] Javier Herrero-Martín et al. In: *Phys. Rev. B* 72 (2005), p. 085106.
[45] Y. Zhang et al. In: *arXiv:1805.09268v1* ().